Published in final edited form as:
Bioconjug Chem. 2011 September 21; 22(9): 1811–1823. doi:10.1021/bc2002117.

Metabolism of diazirine-modified *N*-acetylmannosamine analogs to photocrosslinking sialosides

Michelle R. Bond[†,‡], **Haochi Zhang**[‡], **Jaekuk Kim**[‡], **Seok-Ho Yu**[‡], **Fan Yang**[‡], **Steven M. Patrie**[‡], and **Jennifer J. Kohler**[‡,*]

[†]Department of Chemistry, Stanford University, Stanford, CA 94305

[‡]Division of Translational Research, Department of Internal Medicine, 5323 Harry Hines Boulevard, University of Texas Southwestern Medical Center, Dallas, TX 75390

Abstract

Terminal sialic acid residues often mediate the interactions of cell surface glycoconjugates. Sialic acid-dependent interactions typically exhibit rapid dissociation rates, precluding the use of traditional biological techniques for complex isolation. To stabilize these transient interactions, we employ a targeted photocrosslinking approach in which a diazirine photocrosslinker is incorporated into cell surface sialylated glycoconjugates through the use of metabolic oligosaccharide engineering. We describe three diazirine-modified *N*-acetylmannosamine (ManNAc) analogs in which the length of the linker between the pyranose ring and the diazirine was varied. These analogs were each metabolized to their respective sialic acid counterparts, which were added to both glycoproteins and glycolipids. Diazirine-modified sialic acid analogs could be incorporated into both α2–3 and α2–6 linkages. Upon exposure to UV irradiation, diazirine-modified glycoconjugates were covalently crosslinked to their interaction partners. We demonstrate that all three diazirine-modified analogs were capable of competing with endogeneous sialic acid, albeit to varying degrees. We found that larger analogs were less efficiently metabolized, yet could still function as effective crosslinkers. Notably, the addition of the diazirine substituent interferes with metabolism of ManNAc analogs to glycans other than sialosides, providing fidelity to selectively incorporate the crosslinker into sialylated molecules. These compounds are non-toxic and display only minimal growth inhibition at the concentrations required for crosslinking studies. This report provides essential information for the deployment of photocrosslinking analogs to capture and study ephemeral, yet essential, sialic acid-mediated interactions.

Introduction

Glycans are essential components of the mammalian cell surface, conferring an additional level of complexity to the heterogeneous compilation of proteins and lipids present on the plasma membrane. Glycoconjugates, including both glycoproteins and glycolipids, influence a diverse array of biological processes in eukaryotes, including mediating interactions among cells and between cells and the extracellular matrix. Alpha-keto acidic sugars known as sialic acids are key features of many cell surface glycoconjugates. The presence or absence of these nine-carbon sugars can significantly change the immunogenicity and bioactivity of glycoproteins and glycolipids.[1] Due to their privileged positions at the periphery of glycan structures, sialic acids are also crucial components of recognition elements.[2, 3] For example, sialic acid-containing glycoconjugates are responsible for

*To whom correspondence should be directed. phone: 214-648-1214; fax: 214-648-4156; jennifer.kohler@utsouthwestern.edu.

leukocyte homing to the sites of inflammation[4] and are critical for mediating cellular susceptibility to toxins[5] and viruses.[6]

Although burgeoning evidence points to essential roles for sialylation,[7] studying sialylated glycoconjugates, also called sialosides, remains challenging. Glycan-mediated interactions are often transient and characterized by low affinities with equilibrium dissociation constants typically in the μM to mM range.[4] The diversity and abundance of sialic acid-mediated interactions have yet to be explored fully due to the limited tools available for analyzing these labile complexes. Our strategy for studying a sialoside-mediated interaction is to covalently conjugate the complex via covalent photocrosslinking, thereby capturing the interaction between the binding partners and enabling further analysis. By using metabolic oligosaccharide engineering,[8] a photoreactive moiety is selectively incorporated into sialylated glycoconjugates in their native cellular context. The photocrosslinkers are then poised to capture biologically-relevant complexes.

Metabolically incorporated photocrosslinking sialic acids have been reported by our lab[9] and others[10, 11] and their utility has been demonstrated by the covalent capture of both glycoprotein-glycoprotein [9, 10, 12] and protein-glycolipid[13] interactions. Although several photocrosslinking groups have demonstrated utility in biological settings,[14] we have focused exclusively on the use of the alkyl diazirine. The diazirine is activated by exposure to 365 nm light, whereupon it is converted into a highly reactive carbene intermediate[15] that will insert into any nearby C-H or heteroatom-H bond. The diazirine's small size, high reactivity, and low selectivity offer advantages over other crosslinking moieties.[14]

Previously, we reported the synthesis of a diazirine-modified *N*-acetylmannosamine (ManNAc) analog and showed that this compound could be metabolized to sialosides and used to crosslink a sialylated protein and a sialylated lipid to their binding partners.[9, 13] While we successfully observed crosslinking, we were unsure whether the distance between the pyranose ring and the photocrosslinker was optimal for efficient capture of sialoside binding partners. To address this concern, we prepared a panel of ManNAc analogs in which we varied the distance between the pyranose ring and the photocrosslinker.

Here we report the synthesis of variable-length photocrosslinking ManNAc analogs and the results of their introduction in BJA-B, Daudi, and Jurkat cells. We examined the effects of these compounds on cell viability and growth. We show that these analogs are metabolized to photocrosslinking sialosides, but not to other glycoconjugates. Finally, we compare the ability of the different photocrosslinking sialic acids to covalently capture complexes containing either a sialylated glycoprotein or a sialylated glycolipid. Overall, we found that the compound with the shortest linker displayed the most efficient incorporation, also resulting in effective crosslinking. Compounds with a longer linker between the pyranose ring and the photocrosslinker suffer from poor incorporation, yet are still capable of crosslinking. In studying the metabolism of these analogs, we discovered that the addition of the diazirine modification interferes with interconversion of ManNAc and *N*-acetylglucosamine (GlcNAc) analogs, thereby enabling selective incorporation of the diazirine into sialosides. Finally, we demonstrate that crosslinked complexes can be characterized by self-assembled monolayer (SAM) with matrix-assisted laser desorption/ ionization (MALDI) time-of-flight mass spectrometry, providing a potential route to discovery and characterization of sialoside binding partners.

Experimental Procedures

Chemical synthesis of photocrosslinking sugars

Syntheses of **1–4** have been reported previously.[9, 16, 17] Compounds **5** and **6** were prepared by a route analogous to **4** and described in detail in the Supporting Information. Acetylated sugars were purified by silica gel chromatography and reverse phase HPLC. Synthetic details, NMR spectra, and HPLC traces demonstrating compound purity are found in the Supporting Information (Schemes S1–S3 and Figures S10–S24).

Cell culture, flow cytometry, and immunoblotting

BJA-B K88, BJA-B K20, and Daudi cells were cultivated in RPMI 1640 media containing 2 mM glutamine and supplemented with 10% fetal calf serum, 100 U/mL penicillin, and 100 μg/ml streptomycin. Unless otherwise noted, cells were maintained in a water-saturated atmosphere at 37 °C and 5% CO_2. Typically, cell densities were maintained between 2.5×10^5 and 2.0×10^6. To generate BJA-B cells in serum free conditions, the cells were grown in RPMI 1640 with 2 mM L-glutamine containing 1X Nutridoma SP, 50 U/ml penicillin, and 50 μg/ml streptomycin. Cells were cultured for two passages at 2.5×10^5 cells/mL in serum-free media for 72 h prior to supplementation with monosaccharides.

Prior to the addition of cells to a 12 well plate, ethanol (EtOH), Ac_4ManNAc, Ac_4ManNDAz(2me), Ac_4ManNDAz(3me), Ac_4ManNDAz(4me), Ac_4GlcNDAz(2me), or Ac_4ManNAz in EtOH were added to achieve a final concentration of 100 μM once media was added. EtOH was evaporated at ambient temperature and pressure prior to the addition of cells. Cells were seeded at a density of 3.0×10^5 cells/mL and cultured for 72 h with the compounds. After growth in the presence of the appropriate monosaccharides, cells were harvested by pelleting at 400*g* for 4 min and aspirating the supernatant. Cell viability was assessed using Trypan blue dye staining with the Countness Automated Cell Counter instrument (Invitrogen, Carlsbad, CA). When possible, cells were kept in the dark and on ice for subsequent procedures.

Jurkat cells were cultivated in RPMI 1640 media containing 2 mM L-glutamine and supplemented with 10% heat-inactivated FBS. Unless otherwise noted, cells were maintained in a water-saturated atmosphere at 37 °C and 5% CO_2. Typically, cell densities were maintained between 2.5×10^5 and 2.0×10^6. Cell viability was assessed using Trypan blue dye staining with the Countess Automated Cell Counter.

Flow cytometry and immunoblotting were performed according to reported procedures.[9, 13, 16] Details are provided in the Supporting Information.

Analysis of ganglioside content for Jurkat cells cultured with compounds 1–6

All reagents, chemicals, and general supplies were purchased and used as received from Fisher Scientific (Waltham, MA) or Sigma-Aldrich (St. Louis, MO) unless otherwise noted. Dulbecco's phosphate buffered saline (DPBS) and CTxB-488 were purchased from Invitrogen (Carlsbad, CA). Bovine serum albumin (BSA) Fraction V was purchased from Roche Applied Science (Indianapolis, IN). SepPak tC18 columns (0.3 g) were purchased from Fisher Scientific. HPTLC plates (20 × 20 cm, glass-backed, 200 μm thickness) were purchased from EMD Chemicals (Gibbstown, NJ). Matreya ganglioside standards 1408, 1510, and 1511 were purchased from Matreya LLC (Pleasant Gap, MD).

Jurkat cells were cultivated as described above. Prior to the addition of cells to a 25 cm plate, EtOH, Ac_4ManNAc, Ac_4ManNDAz(2me), Ac_4ManNDAz(3me), Ac_4ManNDAz(4me), Ac_4GlcNDAz(2me), or Ac_4ManNAz in EtOH were added to achieve

a final concentration of 100 μM once the media was added. The EtOH was pre-evaporated at ambient temperature and pressure. Jurkat cells were then seeded at a density of 2.5×10^5 cells/mL and incubated in the presence of the monosaccharides at 37 °C and 5% CO_2. After growth with the appropriate compounds for 72 h, cells were harvested, counted, and centrifuged at 650*g* for 5 min in 50 mL conical tubes and the supernatant aspirated. To ensure that all ganglioside concentrations were normalized, equal numbers of cells (2.7×10^7 cells) were collected for all samples. Cell pellets were stored at −80 °C overnight.

Cell pellets were thawed to RT and resuspended in 300 μL of ice-cold ddH_2O. They were then dounced 50 times with a Kontes tissue grinder, tube size 20. Following homogenization, cell suspension was added to a vial of stirring MeOH (800 μL). For the previous step and those following, glass Pasteur pipettes and glass vials were used; no plastic came in contact with samples. Samples were also shielded from light at every point possible during this procedure. To the stirring solution, 400 μL of chloroform was added and the mixture stirred for 2.5 h at RT. The mixture was then transferred into a 13 × 100 mm glass culture tube and centrifuged at 2800*g* for 10 min at 30 °C. The resulting supernatant (total lipid extract - TLE) was transferred to a glass vial and the sample evaporated under a stream of nitrogen to dryness. The resulting yellow film was stored at RT in the dark.

For ganglioside isolation, the TLE was resuspended in 1200 μL of diisopropyl ether and 800 μL 1-butanol. This mixture was sonicated in a bath sonicator for 10 min. The resulting cloudy solution was transferred to a 13 × 100 mm glass culture tube. To the solution, 1 mL of 50 mM sodium chloride was added. Following mixing with a Pasteur pipette, the suspension was centrifuged at 2800*g* for 10 min at 30 °C to separate the two phases. The upper (organic) layer was then removed. To the aqueous layer, 1200 μL of diisopropyl ether and 800 μL of 1-butanol were added and mixed. Following centrifugation at 2800*g* for 10 min at 30 °C and removal of the organic layer; these last two steps were repeated once more.

For final purification, the remaining lipid mixture was loaded on a SepPak tC18 column (0.3g size), washed and eluted. First, the column was prepared by several washing steps: three washes with 2 mL of chloroform:MeOH:ddH_2O (C:M:W, 2:43:55) were followed by two washes with 2 mL of C:M (1:1) and lastly three more washes with 2 mL of C:M:W (2:43:55). The sample was loaded onto the column and washed thrice with 2 mL of C:M:W (2:43:55) followed by three washes with 2 mL of M:W (1:1). Finally, the gangliosides were eluted in 2 mL of 100% MeOH. Ganglioside extracts were then transferred to a new 4 mL glass vial and evaporated to dryness under a stream of nitrogen. The clear, white film was stored at RT for further analysis.

A TLC chamber was pre-equilibrated with 140 mL of chloroform:MeOH:0.2% $CaCl_{2(aq)}$ (85:45:10). The HPTLC plate (EMD Chemicals #115534, 20 × 20 cm, glass-backed plates, silica gel 60 F_{254}, 200 μm thickness) was pre-run and dried prior to sample loading to improve resolution. The syringe used for loading samples was cleaned with C:M:W, 4:8:3. Extracted ganglioside samples were redissolved in 50 μL C:M:W (2:1:0.1) and loaded onto the HPTLC plate along with ganglioside standards and dried. The HPTLC plate was then run in the chamber followed by drying under vacuum for 45 min.

To assess the presence of GM1a, the HPTLC plate was immersed in 0.5% polyisobutylmethacrylate in hexanes (diluted from a stock solution of 2% in chloroform) for 2 min to fix the gangliosides to the TLC plate. The plate was then fully dried followed by immersion in 1.0% BSA in DPBS for 30 min at RT. The plate was incubated with CTxB-Alexa Fluor 488 conjugate (1:20,000 dilution of a 1 mg/mL solution) in DBPS for 50 min at RT in the dark. The plate was washed briefly with DPBS, dried fully, and imaged by

Typhoon with a 488 nm excitation laser and 520 nm emission filter. Global adjustments to image contrast and brightness were performed using Adobe Photoshop.

To visualize all gangliosides, the above plate was resorcinol-stained. The plate was sprayed with a resorcinol solution (0.1% resorcinol, 0.04% $CuSO_4$ in hydrochloric acid: water (4:1)). Following staining, the plate was thoroughly dried and sandwiched between two glass plates, then incubated at ~100 °C for 15–20 min until bands were clearly visible. The plate was imaged with white light using an Alpha Innotech FluorChem HD2 imager and global adjustments to image contrast and brightness were made with Adobe Photoshop.

Cytosolic and membrane-bound sialic acid analysis by DMB derivatization

All reagents, chemicals, and general supplies were purchased and used as received from Fisher Scientific (Waltham, MA) or Sigma-Aldrich (St. Louis, MO) unless otherwise noted. PVDF membranes were purchased from Millipore, Immobilon (Billerica, CA). For chemiluminescent visualization, SuperSignal WestPico Chemiluminescent Substrate (ECL reagent) was purchased from Pierce (Rockford, IL). Polycarbonate centrifuge tubes (11 × 34 mm) were purchased from Beckman (Brea, CA). The bicinchoninic acid (BCA) Protein Assay Kit from Pierce was used to assess protein concentration. DMB was purchased from Sigma Aldrich (we found other vendors' products to be inferior). Amicon Ultra Centrifugal Filters (0.5 mL; 10 kDa molecular weight cut-off (MWCO)) were purchased from Millipore. Complete™ Protease Inhibitor Cocktail Tablet, EDTA-free were purchased from Santa Cruz Biotechnology. Tris-buffered saline Tween-20 was used in blocking solutions (TBST: 10 mM Tris•HCl pH 8.0, 150 mM NaCl, 0.1% v/v Tween 20). The hypotonic lysis buffer was composed of 10 mM Tris•HCl pH 7.3, 10 mM $MgCl_2$, 1 mM EDTA, and 1 mM EGTA.

Jurkat cells were grown in the presence of sugars **1–6** as described above. Cells were harvested after 72 h and the number of cells normalized to 5 million. Cells were washed twice in 500 μL DPBS. Next, cells were swollen in hypotonic lysis buffer containing protease inhibitors for 15 min on ice. Cells were lysed by extrusion through a 25 gauge needle 30 times. Nuclei and unbroken cells were removed from the post-nuclear supernatant by two rounds of centrifugation at 1000*g* for 15 minutes at 4 °C. Next, the post-nuclear supernatant was transferred to heavy-walled polycarbonate tubes and centrifuged at 100,000*g* for 1 h in a Beckman TLA 120.2 rotor. The supernatant was designated the cytosolic fraction. The pellet was washed twice with cold 400 μL hypotonic lysis buffer and centrifuged at 100,000*g* for 1 h. The remaining pellet was designated the membrane fraction. Samples were either flash-frozen and the solvent removed by vacuum overnight or saved to assess fraction purity. To confirm that the membrane fraction was not contaminated by the nuclear fraction, protein concentration was normalized and proteins were resolved by SDS-PAGE. Proteins were then transferred to PVDF and probed for either lamin B (to identify the nuclear fraction) or calnexin (to identify the membrane fraction). DMB-derivatization (as described below) confirmed that no sialic acids were present in the membrane washes; this ensured that that no soluble sialic acid (free sialic acid or CMP-sialic acid) remained in the membrane fraction.

To release sialic acids, 50 or 100 μL of 2.0 M acetic acid was added for the membrane-bound and dried cytosolic samples, respectively. Solutions were incubated at 80 °C for 2 h. Samples were then cooled to room temperature. To the membrane-bound and cytosolic samples, 40 or 80 μL of 7 mM DMB, 0.75 M 2-mercaptoethanol, 18 mM $Na_2S_2O_4$, 1.4 M acetic acid were added, respectively. The samples were then incubated at 50 °C for 2 h. After this incubation period, 5 or 10 μL of 0.2 M NaOH was added to each membrane-bound or cytosolic sample, respectively. Samples were then filtered in 10 kDa MWCO filters by centrifugation and the resulting flow-through was stored at −20 °C, in the dark

until used. The derivatives were analyzed by on-line fluorescence detection using reverse-phase HPLC. Details are provided in the Supporting Information.

Mass spectrometry analysis of crosslinked CTxB-GM1a-SiaDAz(2me)

Photocrosslinking of CTxB-GM1a complexes was performed essentially as described previously.[13] The SAMDI mass spectrometry process was based on a literature procedure.[18] Details are provided in the Supporting Information.

Results

Preparation of photocrosslinking compounds and control molecules

Previously, we reported the synthesis of Ac_4ManNDAz(2me) (**4**), a precursor to photocrosslinking sialosides.[9] Using a similar synthetic scheme (Scheme S1 and details in Supporting Information), we prepared two additional analogs, **5** and **6**, in which the distance between the pyranose ring and the photocrosslinker was extended (Figure 1). In all cases, we prepared per-*O*-acetylated forms of the compounds. Acetylation of hydrophilic sugars improves passive diffusion through the plasma membrane[19] after which the acetyl groups are presumably removed by nonspecific esterases within the cytosol.[20]

Further metabolism of the photocrosslinking compounds relies on the cells' endogenous machinery for biosynthesis of sialosides and the expression levels of each of the required enzymes (Figure 2). ManNAc, the first committed intermediate in sialic acid biosynthesis, is produced from UDP-GlcNAc by the action of the UDP-GlcNAc 2-epimerase. In addition, human cells also encode a GlcNAc 2-epimerase that is capable of interconverting GlcNAc and ManNAc, although the equilibrium favors the more stable GlcNAc.[21] Theoretically, the GlcNAc 2-epimerase could be capable of converting our photocrosslinking ManNAc analogs to their GlcNAc counterparts, which might lead to photocrosslinker incorporation into non-sialylated molecules such as *O*-GlcNAc-modified proteins or glycosaminoglycans. To confirm that any crosslinking we observe is due to diazirine-modified sialosides, as opposed to other possible diazirine-modified molecules, we use Ac_4GlcNDAz(2me) (**3**), the diazirine-modified analog of GlcNAc, as a control molecule. If crosslinking is observed with **4**, but not with **3**, we conclude that the crosslinking is through a diazirine-modified sialoside, not another metabolite.

Maximizing sialoside production while minimizing growth inhibition

We sought to define conditions under which these new photocrosslinking ManNAc analogs are efficiently metabolized to cell surface sialosides. In these initial experiments, we used a cell line that is deficient in sialic acid production. BJA-B K20 cells are a subclone of the BJA-B B-cell lymphoma cell line and are distinguished by their deficiency in UDP-GlcNAc 2-epimerase activity.[22, 23] Because BJA-B K20 cells lack the enzymatic activity required to convert UDP-GlcNAc to ManNAc, they cannot biosynthesize ManNAc or its metabolite sialic acid (Figure 2) from the UDP-GlcNAc precursor. Like many other cells, BJA-B K20 cells are capable of scavenging sialic acids from the culture medium. However, due to their inability to synthesize ManNAc, BJA-B K20 cells cultured in serum-free conditions fail to produce sialosides. If a ManNAc analog is added to this deficient cell line, its metabolic conversion to sialic acid can be assessed by quantifying the total amount of sialic acids present in the cell. In addition to measuring sialoside formation in response to addition of diazirine-modified compounds, we cultured BJA-B K20 cells with the per-*O*-acetylated form of ManNAc (**1**), which we expect to be converted to sialosides effectively, and quantified cell surface sialylation. We also measured sialoside production due to Ac_4ManNAz (**2**),[17] an azide-modified analog that is metabolized to sialosides with high

efficiency.[24] Finally, we examined sialoside production in another BJA-B subclone, K88, which maintains UDP-GlcNAc 2-epimerase activity and has a high sialylation phenotype.[22]

First, we assessed the effects of protected ManNAc analogs on cell growth. BJA-B K20 cells were cultured in serum-free medium with **1**, **2**, **3**, **4**, **5**, or **6** at a range of concentrations, from 10 μM to 300 μM, for 72 h, after which Trypan blue staining was used to assess cell growth and viability. For all three photocrosslinking ManNAc analogs, increases in analog concentration correlated with decreased cell numbers (Supporting Information, Figure S1). The most dramatic example is the case of Ac_4ManNDAz(4me), where 45% fewer cells were observed when 300 μM compound was added to the culture, versus 10 μM compound. In contrast, when cells were supplemented with Ac_4ManNAz and Ac_4GlcNDAz(2me), the number of cells remained similar regardless of sugar concentration. Despite these different trends, relatively little growth inhibition was observed for any compound added at 100 μM. We also assessed cell viability using Trypan blue staining. We did not observe any significant viability trends and the fraction of live cells was high (86–94%) for all samples (Supporting Information, Figure S1). These data suggest that higher concentrations of the unnatural sugar analogs are detrimental to cell growth but do not significantly affect cell viability.

After assessing cell viability, we monitored the level of cell surface α2–6-linked sialic acids resulting from supplementation with compounds **1–6**. We used a fluorescently labeled *Sambucus nigra* agglutinin (SNA) conjugate (SNA-FITC) to measure production of cell surface α2–6-linked sialic acids. In the sialic acid-deficient BJA-B K20 cell line, essentially all of the sialic acids are derived from the exogenous addition of ManNAc analogs. Importantly, the SNA lectin tolerates deviations in the *N*-acyl side chain, so the diazirine modification is not expected to affect SNA binding.[25, 26] For cells treated with Ac_4ManNAc, cell surface α2–6-linked sialic acid increased robustly, even at 10 μM (Figure 3). Cells treated with Ac_4ManNDAz(2me) and Ac_4ManNAz also displayed relatively high levels of cell surface α2–6-linked sialic acids. Conversely, to rise above the BJA-B K20 baseline level, cells cultures with Ac_4ManNDAz(3me) or Ac_4ManNDAz(4me) required sugar concentrations of 50 or 100 μM. BJA-B K20 cells treated with Ac_4GlcNDAz(2me) showed no increase in cell surface sialic acid, indicating that conversion of GlcNDAz(2me) to ManNDAz(2me) is negligible. These data, along with the growth data (Figure S1), led us to choose 100 μM as an optimal concentration of photocrosslinking sugar to maximize incorporation while minimizing growth inhibition.

N-acyl side chain length is negatively correlated with incorporation efficiency

To measure the total amount of cell surface photocrosslinking sialic acid, we used the *p*eriodate oxidation and *a*niline-catalyzed oxime *l*igation (PAL) with flow cytometry detection essentially as reported by the Paulson lab.[27] In brief, photocrosslinking sugar-supplemented cells were treated with sodium periodate to oxidize the polyol chain of cell surface sialic acids to an aldehyde, a functional group that is otherwise absent from the cell surface. We used an *in vitro* reaction to confirm that this oxidation reaction had no effect on the diazirine functionality (Figure S2). Oxidized cells were incubated with an aminooxy-biotin reagent in the presence of aniline catalyst, yielding cell surface sialic acids covalently conjugated to biotin through an oxime linkage. Finally, streptavidin-DTAF was added, yielding fluorescence labeling proportional to cell surface sialic acid. Fluorescence was quantified by flow cytometry (Figure 4A).

After PAL labeling, those cells with an intact sialic acid pathway (BJA-B K88) showed a much higher level of fluorescence than the BJA-B K20 cells that lack UDP-GlcNAc 2-epimerase activity (Figure 4A). Similarly, in comparison to unsupplemented BJA-B K20 cells, there was a marked increase in fluorescence for those BJA-B K20 cells incubated with

certain ManNAc analogs. Our results demonstrate a robust conversion of Ac_4ManNDAz(2me) to cell surface sialic acid, similar to the levels seen for Ac_4ManNAc and Ac_4ManNAz. Conversion of Ac_4ManNDAz(3me) to the corresponding sialosides was demonstrated by the increase of fluorescence to slightly above baseline levels. Treatment with Ac_4ManNDAz(4me) did not yield a detectable increase in cell surface sialic acid. As expected, cells treated with the Ac_4GlcNDAz(2me) control molecule displayed little difference from unsupplemented BJA-B cells, reflecting their inability to produce ManNDAz(2me) from Ac_4GlcNDAz(2me). These data are supported by results of a resorcinol assay (described in the Supporting Information) used to determine levels of total and glycoconjugate-bound sialic acids (Figure S3).

Photocrosslinking sialic acids are incorporated in a variety of glycans

After confirming that photocrosslinking ManNAc analogs are metabolized to cell surface sialic acids, we next examined whether our analogs were incorporated as both α2–3-linked and α2–6-linked sialic acids. We assessed the cell surface binding of lectins, proteins that recognize specific sugar epitopes, by flow cytometry. We used labeled SNA[28] and *Maackia amurenis* lectin (MAL-II)[29, 30] which recognize Sia α2–6Gal and Sia α2–3Gal, respectively. For these experiments, BJA-B K20 cells were unsupplemented or cultured with 100 μM **1–6**, as described in the Supporting Information. Cells were washed and labeled with the appropriate lectins and their fluorescence assessed by flow cytometry.

Unsupplemented BJA-B K20 cells bound SNA and MAL-II at low levels (Figure 4B and 4C), unlike the BJA-B K88 cells, which bound both lectins at high levels. Culturing BJA-B K20 cells with Ac_4ManNAc yielded a dramatic increase in SNA and MAL-II binding whereas culturing the cells with Ac_4GlcNDAz(2me) yielded no increase in lectin binding. When BJA-B K20 cells were supplemented with the unnatural photocrosslinking ManNAc analogs, only those cultured with Ac_4ManNDAz(2me) showed significant levels of binding to MAL-II, while cells cultured with either Ac_4ManNDAz(2me) or Ac_4ManNDAz(3me) bound to SNA. No detectable increases in lectin binding were observed for cells cultured with Ac_4ManNDAz(4me).

Although published data suggest that *N*-acyl substituents to sialic acid do not affect SNA or MAL-II binding,[26] we remained concerned that the lack of sialoside production we observed for the larger analogs could reflect lower affinity of the lectins to the modified sialic acids. To provide complementary information on the degree of sialylation, we also tested the binding of fluorescently conjugated lectins recognizing core glycan structures. The lectins used were: *Erythrina cristagalli* agglutinin (ECA, specific for terminal LacNAc)[31] and *Helix pomatia* lectin (HPA, specific for terminal GalNAc).[32] Addition of sialic acid would be predicted to mask these core glycans, resulting in decreased lectin binding. Unsupplemented BJA-B K20 cells were bound by ECA and HPA at high levels (Figure 4D and 4E); BJA-B K88 cells bound the same lectins at lower levels. Culturing BJA-B K20 cells with Ac_4ManNAc yielded sharp decreases in ECA and HPA lectin binding. Cells cultured with Ac_4ManNDAz(2me) also displayed decreases in ECA and HPA binding, but cells cultured with Ac_4ManNDAz(3me) or Ac_4ManNDAz(4me) did not show dramatic changes. Culturing BJA-B K20 cells with Ac_4GlcNDAz(2me) had no effect on ECA or HPA binding. Taken together, our cell surface binding data provide strong evidence for the metabolism of Ac_4ManNDAz(2me) to both α2–6-linked and α2–3-linked sialic acids, and for the metabolism of Ac_4ManNDAz(3me) to at least α2–6-linked sialic acids. None of the flow cytometry data provide definitive evidence for metabolism of 100 μM Ac_4ManNDAz(4me) to cell surface sialic acid.

Photocrosslinking sialic acids crosslink a sialylated glycoprotein

To confirm the utility of our photocrosslinking sugar analogs, we captured a known sialic acid-mediated protein interaction and visualized the complex by immunoblot. The sialic acid binding *Ig*G-like *lec*tin (Siglec) CD22 is a protein that is not only modified by α2–6-linked sialic acid but it also binds sialic acid attached to other molecules, including other copies of CD22.[10, 12] Several studies have demonstrated crosslinking of CD22 mediated by unnatural sialic acids.[9, 10, 12, 14] Here we monitored CD22 crosslinking in two different B cell lines: BJA-B K20 and Daudi. Using BJA-B K20 cells in serum free media, we expected to observe high levels of crosslinking, since the photocrosslinking sialic acid analogs do not need to compete with endogenous sialic acid for incorporation into sialosides. We cultured cells in the presence of the unnatural sugar analogs, photoirradiated the cells, and harvested the cell lysates. Lysates were resolved by denaturing sodium dodecyl sulfate polyacrylamide gel electrophoresis (SDS-PAGE), transferred to a polyvinylidine fluoride membrane (PVDF), and probed for the presence of CD22.

Monomeric CD22 displays an apparent molecular weight of ~120 kDa; a shift to higher molecular weight is indicative of production of a photocrosslinked product (Figure 5A). As shown previously,[9] we observed photocrosslinking of CD22 when cells were cultured with Ac_4ManNDAz(2me). Cells cultured with Ac_4ManNDAz(3me) or Ac_4ManNDAz(4me) also produced crosslinked species, although the amount of photocrosslinked product was less. Cells cultured with Ac_4GlcNDAz(2me) produced no photocrosslinked product, consistent with our hypothesis that photocrosslinking occurs through sialic acid, not other metabolites of the diazirine-modified sugars. Importantly, appearance of the putative crosslinked species was both UV- and diazirine-dependent. Lysates from cells that were not photoirradiated produced no bands other than monomeric CD22 (Figure 5B). All blots were stripped and reprobed for β-actin to demonstrate similar protein loading in every lane (data not shown).

The utility of photocrosslinking sialic acid analogs will be limited if they can only be used in cell lines that are deficient in sialic acid synthesis. Therefore, we next tested whether the larger photocrosslinking ManNAc analogs could engender sialoside crosslinking in cells that contain endogenous sialic acid. For these experiments, we analyzed CD22 crosslinking in the Daudi B cell line. When photoirradiated, only cells supplemented with Ac_4ManNDAz(2me) showed an anti-CD22 reactive band of increased molecular weight, corresponding to crosslinked CD22 (Figure 5C). Lysates from Daudi cells cultured with Ac_4ManNDAz(3me) or Ac_4ManNDAz(4me) did not display crosslinked CD22 even upon long exposures, suggesting inadequate competition with endogenous sialic acid. Lysates from Daudi cells not exposed to UV light did not reveal any crosslinked product (Figure 5D). Notably, Ac_4GlcNDAz(2me)-treated cells produced no photocrosslinked product after UV exposure. These data suggest that Ac_4GlcNDAz(2me) is not metabolized to a photocrosslinking sialic acid analog even though Daudi cells have UDP-GlcNAc 2-epimerase activity and are therefore capable of converting UDP-GlcNAc to ManNAc.

Photocrosslinking sialic acids compete with Neu5Ac for incorporation into glycoconjugates

Having obtained indirect evidence that at least one photocrosslinking sialic acid can compete with endogenous sialic acids, we wished to quantify the efficiency of photocrosslinking sialic acid metabolism. We conducted this assessment in the Jurkat T cell line, because previous work indicated that sialic acid analogs can compete efficiently with Neu5Ac in this cell line.[24] We cultured Jurkat cells for 72 hours with **1**, **3**, **4**, **5**, or **6**, then harvested the cells and fractionated them into cytosolic and membrane components. Cytosolic fractions should contain primarily free sialic acids and CMP-sialic acids, while the membrane fractions contain sialic acids that have been incorporated into glycoconjugates.

Each sample was subjected to mild acid hydrolysis to release ketosidically-linked sialic acids and then treated with 1,2-diamino-4,5-methylenedioxybenzene (DMB) to fluorescently derivatize the sialic acids. Separation by reverse phase HPLC and fluorescence detection[24, 33, 34] enabled us to quantify the ratios of sialic acids present in each sample (raw data shown in Figures S4–S6).

Jurkat cells cultured in the absence of exogenous ManNAc analogs or in the presence of compounds **1** and **3** contained a single form of naturally occurring sialic acid, Neu5Ac (Table 1). Cells cultured with 100 μM Ac_4ManNDAz(2me) also contained significant quantities of a novel sialic acid species. Comparison of the retention time and mass to standard molecules revealed that this species is the sialic acid metabolite of Ac_4ManNDAz(2me), which we name SiaDAz(2me). SiaDAz(2me) comprised a greater portion of the total sialic acid in the cytosolic fraction (85%) than in the membrane fraction (74%). As expected from the crosslinking data, larger sialic acid analogs were less competitive with Neu5Ac. Supplementation with Ac_4ManNDAz(3me) yielded another novel peak, whose retention time and mass matched that of DMB-SiaDAz(3me) (**19**, Scheme S2), but it comprised only about a third of the cytosolic sialic acid and less than 10% of the membrane-associated sialic acid. We were unable to detect a sialic acid corresponding to SiaDAz(4me) in the lysates from cell supplemented with Ac_4ManNDAz(4me).

Taken together, the DMB derivatization data indicate that SiaDAz(2me) is efficiently incorporated into sialic acid-containing glycoconjugates, effectively replacing up to 74% of the cell surface Neu5Ac in Jurkat cells. Further, these results confirm that larger photocrosslinking ManNAc analogs are less efficiently metabolized to sialic acid and to cell surface sialosides. Finally, our data indicate that the photocrosslinking sialic acids are better represented among cytosolic sialic acids than among membrane sialic acids.

N-acyl diazirine restricts ManNAc-GlcNAc crosstalk

Next, we wished to examine whether diazirine-modified ManNAc could be metabolized to glycans other than sialosides. In cells, ManNAc is synthesized from UDP-GlcNAc by the UDP-GlcNAc 2-epimerase. While the reverse reaction is disfavored, a second enzyme, GlcNAc 2-epimerase, is capable of interconverting ManNAc and GlcNAc.[21] Therefore, the activity of GlcNAc 2-epimerase could potentially lead to incorporation of diazirine crosslinkers into GlcNAc-containing glycans, rather than sialic acid-containing glycans. To investigate this possibility, we cultured Jurkat cells with 100 μM Ac_4ManNDAz(2me), 100 μM Ac_4GlcNDAz(2me), or no exogenous sugar. After 72 hours, the cells were harvested and lysed. Cell lysates were examined by high performance anion exchange chromatography (HPAEC) to identify diazirine-containing nucleotide-sugar donors. As shown previously,[35] Jurkat cells cultured with Ac_4ManNDAz(2me) produce a new species, whose retention time is slightly longer than that of CMP-Neu5Ac (Figure S7). This new species is UV-sensitive and is therefore assigned as CMP-SiaDAz(2me). Notably the CMP-SiaDAz(2me) peak was not observed in lysates from untreated Jurkat cells or from cells cultured with Ac_4GlcNDAz(2me). Next, we looked for evidence of UDP-GlcNDAz(2me) in the Jurkat lysates. None of the lysates displayed a peak with a retention time matching that of synthetic UDP-GlcNDAz(2me) (Scheme S3 and Figure S8). These results imply that the diazirine crosslinker is specifically directed toward incorporation into sialosides and not into other glycans.

Photocrosslinking sialic acids are incorporated into gangliosides

Our CD22 photocrosslinking experiments in BJA-B K20 cells indicated that the larger photocrosslinking ManNAc analogs were metabolized to sialic acids and incorporated into sialic acid-containing glycoproteins. We next tested if the new photocrosslinking sialic acids

could also be incorporated into sialic acid-containing glycolipids, as has been shown for other sialic acid analogs.[13, 36–41] Briefly, Jurkat cells were cultured in the presence of sugars **1–6** for 72 hours. After harvesting the cells, a series of extractions were employed to remove insoluble membrane components, proteins, phospholipids, and uncharged lipids.[42, 43] Next, the resulting ganglioside fraction was separated by high-performance thin layer chromatography (HPTLC). The resolved sialylated lipids were detected using resorcinol staining. Resorcinol selectively reacts with sialic acid to yield grey-blue bands; asialo species appear brown. As we have observed previously,[13] Jurkat cells produce multiple gangliosides, identified as GD1a, GM1a, GM2, and GM3 based on their mobilities in comparison to standards (Figure 6A). Due to two different fatty acid chain lengths, the Jurkat gangliosides run in pairs. Resorcinol staining revealed a change in banding pattern for only two samples, corresponding to cells supplemented with Ac_4ManNDAz(2me) or Ac_4ManNAz (Figure 6A). Novel bands appearing in these lanes displayed R_f values higher than those in the control lanes; we interpret the addition of these to correspond to the production of diazirine- and azido-modified gangliosides, respectively. We previously confirmed the identity of the SiaDAz(2me)-modified gangliosides by matrix-assisted laser desorption ionization time-of-flight (MALDI-TOF) MS analysis.[13] Resorcinol staining did not provide evidence for SiaDAz(3me) or SiaDAz(4me) incorporation into gangliosides.

CTxB-488 recognizes GM1a analogs modified by photocrosslinking sialic acids

We next interrogated the ganglioside composition of these lysates using Alexa Fluor 488-labeled cholera toxin subunit B (CTxB-488) to probe the HPTLC plates. This analysis is about 1000 times more sensitive than resorcinol staining (Figure S9). We found that CTxB-488 efficiently bound natural GM1a in all Jurkat cell extracts (Figure 6B). Importantly, CTxB-488 also recognized additional species in extracts from cells supplemented with Ac_4ManNDAz(2me), Ac_4ManNDAz(3me), and Ac_4ManNAz, suggesting that SiaDAz(2me), SiaDAz(3me), and SiaNAz are each incorporated into GM1a gangliosides. We did not observe CTxB-488 binding to any additional species in the lane corresponding to Ac_4ManNDAz(4me)-treated cells, indicating that GM1a-SiaDAz(4me) was not produced at detectable levels or that the larger modification interferes with CTxB binding. In addition to confirming unnatural ganglioside production, these results provide evidence that CTxB can recognize and bind diazirine-modified ganglioside species.

Photocrosslinking sialic acid covalently traps the GM1a-CTxB complex

Previously, we showed that SiaDAz(2me)-modified GM1a could be crosslinked to CTxB.[13] To determine if other diazirine-modified GM1a molecules could be used to covalently capture a ganglioside-protein complex, we cultured Jurkat cells with per-*O*-acetylated ManNAc analogs, incubated the cells with CTxB, and then irradiated the cells with 365 nm light for 45 min. Cells were lysed using a Triton X-100-based lysis buffer and the proteins separated by SDS-PAGE under reducing conditions. Separated proteins were transferred to a PVDF membrane and probed for the presence of CTxB by standard protein immunoblotting techniques. When Jurkat cells were cultured with Ac_4ManNDAz(2me) and Ac_4ManNDAz(3me), we observed a new species whose mobility was slightly slower than CTxB (~11.6 kDa), consistent with the covalent addition of a GM1a molecule (~1.5 kDa) forming a ~13 kDa complex (Figure 7A). Surprisingly, a modest amount of this lower mobility species was also observed in lysates from cells cultured with Ac_4ManNDAz(4me) or Ac_4ManNAz, suggesting that both the poorly incorporated SiaDAz(4me) and the inefficient crosslinker SiaNAz are each capable of mediating GM1a-CTxB crosslinking. In contrast, lysates from cells cultured with no compound, Ac_4ManNAc, or Ac_4GlcNDAz(2me) displayed a single band corresponding to unmodified CTxB. In complementary experiments, we probed membranes for the presence of GM1a with horseradish peroxidase-conjugated CTxB (CTxB-HRP). We observed GM1a present in all

samples. For cells cultured with Ac_4ManNDAz(2me), we also observed an additional species that had a mobility consistent with crosslinked CTxB-GM1a-SiaDAz(2me) (Figure 7C). The intensity of the crosslinked band detected by CTxB-HRP is much less than that observed in the anti-CTxB blot; the source of the difference is not clear, but may reflect the fact that only a small fraction of GM1a is engaging in CTxB crosslinking, or that crosslinked GM1a is not strongly recognized by CTxB-HRP. Given the low intensity of the crosslinked CTxB-GM1a-SiaDAz(2me) detected by CTxB-HRP, it was not surprising that we did not observe crosslinked bands in any other lanes. Importantly, cells that were not exposed to 365 nm light revealed no formation of the CTxB-GM1a complex, demonstrating that complex formation was UV-dependent (Figure 7B and 7D). Furthermore, samples from Ac_4ManNAc-treated cells do not reveal any species with increased molecular weight, indicating that complex formation is dependent on the presence of a photo-reactive moiety.

To solidify our assignment of the CTxB-GM1a-SiaDAz(2me) complex, we used self-assembled monolayer (SAM) with matrix-assisted laser desorption/ionization (MALDI) time-of-flight mass spectrometry (denoted SAMDI-TOF-MS) analysis of cell lysates. A detailed description of the analysis is provided in the Supporting Information. This procedure directly immunoprecipitates the CTxB and CTxB-GM1a-SiaDAz(2me) species onto the gold chip followed by molecular weight determination of the bound analytes. Briefly, gold chips bearing NTA-based SAMs were first treated with $NiSO_4$ to generate the NTA/Ni^{2+} complex and then functionalized with His_6-tagged protein G followed by a rabbit anti-CTxB antibody.[18] These antibody-treated chips were then incubated with cell lysates, which were generated as described for the immunoblotting experiments. After washing the SAM chips, α-cyano-4-hydroxycinnamic acid (CHCA) matrix was deposited on top of the chips followed by MALDI-TOF MS analysis.

SAMDI experiments on lysates from cells cultured in the presence of Ac_4ManNAc revealed a molecular ion that corresponded to the singly charged monomeric CTxB (Figure 7E).[44, 45] For the sample derived from cells cultured with Ac_4ManNDAz(2me), a second molecular ion at 1555 Da higher molecular weight was observed. This mass difference correlates (within experimental error) to the addition of the GM1a-SiaDAz(2me) (1557 Da) to CTxB (Figure 7F) and thus confirms the assignment of the covalently captured CTxB-GM1a-SiaDAz(2me) species in the immunoblot (Figures 7A and 7C).

Discussion

Factors affecting conversion of photocrosslinking sugars to sialosides

Here we investigated the metabolism of three photocrosslinking ManNAc analogs of varying sizes. We discovered that each of these compounds could be metabolized to their sialic acid counterparts, incorporated into cellular sialosides, and employed to crosslink sialoside complexes. Consistent with previous reports,[11, 46, 47] we found that the size of the *N*-acyl chain modification was inversely correlated with the metabolism efficiency. Indeed, for the largest diazirine-modified sugar, detection of SiaDAz(4me)-containing glycoconjugates was difficult: we were only able to infer their presence from the CD22 crosslinking that we observed in BJA-B K20 cells and the CTxB-GM1a crosslinking that we observed in Jurkat cells. DMB derivatization of sialic acids present in the soluble, cytoplasmic fraction revealed that *N*-acyl chain length discrimination is a feature of one or more of the cytosolic or nuclear enzymes involved in converting the ManNAc analogs to sialic acid and CMP-sialic acid analogs. This finding is consistent with previous reports that ManNAc 6-kinase functions as a bottleneck for unnatural sialoside production.[46] Indeed, others have found that the use of sialic acid analogs, rather than ManNAc analogs, can offer a strategy to bypass restrictions on the types of sialosides that can be produced.[11, 48] In addition, we observed that the fractional representation of the unnatural photocrosslinking

sialic acids is lower in the membrane fraction, as compared to the cytosolic fraction. While some of this difference might arise from a system that has not achieved equilibrium, we hypothesize that it could also reflect additional discrimination against the unnatural sialic acids, either at the level of transport of the CMP-sialic acids into the Golgi or tolerance for the CMP-sialic acids by various sialyltransferases.

Metabolic production of unnatural sialosides typically relies on the exogenous addition of ManNAc analogs, since the enzymes involved in the conversion of ManNAc to sialosides (Figure 2) have a well-documented tolerance in their substrate specificity.[8] Human cells can synthesize ManNAc from UDP-GlcNAc, by the action of UDP-GlcNAc 2-epimerase, but are also capable of directly interconverting ManNAc and GlcNAc, through the action of GlcNAc 2-epimerase, provided that this enzyme is expressed.[21] Therefore, GlcNAc analogs could theoretically be converted to ManNAc analogs and, further, to sialosides. However, none of our data indicated that Ac_4GlcNDAz(2me) could be metabolized to SiaDAz(2me), even in Daudi and Jurkat cells, which have UDP-GlcNAc 2-epimerase activity. Using Ac_4GlcNDAz(2me), we saw no evidence of photocrosslinked species (Figures 5 and 7), no additional bands corresponding to a modified GM1a species (Figure 6), and no evidence of SiaDAz(2me) by DMB derivatization. Moreover, our HPAEC data indicated that not only is Ac_4GlcNDAz(2me) not converted to CMP-SiaDAz(2me), but also that Ac_4ManNDAz(2me) is not converted to UDP-GlcNDAz(2me) (Figures S7 and S8). In contrast, when Bertozzi and colleagues studied the metabolism of the smaller, azide-containing molecule Ac_4GlcNAz, they observed metabolism of GlcNAz to SiaNAz.[49] Our results suggest that large substituent found on Ac_4GlcNDAz(2me) restricts entry into the sialic acid biosynthetic pathway and may provide a way to minimize crosstalk between strategies aimed at metabolic labeling of different classes of glycoconjugates. It is important to note that the metabolic fate of ManNAc analogs may vary in different cell lines, depending on the expression of different metabolic enzymes (Figure 2); we did not investigate those expression levels here.

Relationship between incorporation and photocrosslinking efficiencies

Our initial hypothesis was that introducing a longer, flexible linker between the pyranose ring and the diazirine might enhance crosslinking by allowing the crosslinker to sample a larger space. We were unable to test this hypothesis directly, because we found that analogs with longer linkers suffered from relatively poor metabolism to sialosides. Our data indicate that all three photocrosslinking sugars – Ac_4ManNDAz(2me), Ac_4ManNDAz(3me), and Ac_4ManNDAz(4me) – are metabolized to effective photocrosslinking sialosides, but the efficiency of metabolism limits the utility of the two larger compounds. We observed that the largest photocrosslinking analog, Ac_4ManNDAz(4me), yielded CD22 crosslinking in BJA-B K20 cells, but not Daudi cells (Figure 5). Given the poor efficiency of SiaDAz(4me) incorporation, we were surprised to observe CTxB-GM1a crosslinking in Jurkat cells that had been cultured with Ac_4ManNDAz(4me). This result indicates that the small amount of SiaDAz(4me) that is incorporated into GM1a is effective at crosslinking to CTxB and suggests that the diazirine crosslinker in SiaDAz(4me) is well-positioned for capturing this particular sialic acid-mediated interaction. Also surprising was the modest CTxB-GM1a crosslinking that we observed for Jurkat cells cultured with Ac_4ManNAz. Although Ac_4ManNAz is metabolized readily and incorporated into glycoconjugates with high efficiency,[24] we did not expect to observe crosslinking, since alkyl azides are poor photocrosslinking moieties.[50]

Targeting unnatural sialic acids to sectors of the sialome may prove challenging

Sialosides are a diverse set of molecules. Addition of sialic acid to glycoconjugates is catalyzed by one of the twenty sialyltransferases encoded in the human genome.[51, 52]

Although some functional redundancy exists within this family of enzymes, individual members exhibit divergent substrate specificities. Sialyltransferases can add sialic acid to both glycoproteins and glycolipids. Furthermore, sialic acids can be attached in α2–3, α2–6, or α2–8-linkages to a wide variety of underlying glycan structures. Although there are many examples of unnatural sugar incorporation into cellular sialosides,[8] there has been no systematic study to examine the unnatural substrate tolerance of individual sialyltransferases. We wondered whether differences in sialyltransferase specificity would enable selective incorporation of unnatural sialic acids into a particular subset of sialosides. When we examined the incorporation of our three photocrosslinking sialic acid analogs, we found that the overall incorporation levels mirrored the efficiency of incorporation into glycolipids. Similarly, overall incorporation and incorporation into specific linkages and onto specific glycans displayed the same trends. While Golgi-resident sialyltransferases may collectively discriminate against diazirine-modified sialic acid analogs, none of the data presented here suggest that individual sialyltransferases differ in their discrimination patterns.

Achieving sialoside-specific incorporation may require other strategies. Turnover rates for both glycoproteins and glycolipids can vary dramatically,[53, 54] suggesting that the optimal time for analysis of specific species may differ. Perhaps time-dependent metabolic labeling experiments could offer a way to selectively introduce unnatural sialic acids into a particular sector of the sialome. Alternatively, production of an orthogonal mutant sialyltransferase and nucleotidesugar donor could also provide a directed incorporation strategy.

Conclusion

In summary, we described two new diazirine-modified sialic acid precursors, and compared them to a previously reported molecule with respect their efficiency of incorporation into sialosides and their ability to photocrosslinking two glycan-mediated interactions. All three diazirine-modified sialic acid precursors were incorporated into both glycoproteins and glycolipids. We found that the smallest diazirine-modified sialic acid precursor was most efficiently metabolized and competing well with endogenous sialic acid, resulting in up to 74% of cell surface sialic acid being diazirine-modified. We observed that even poorly incorporated analogs could function as crosslinkers. Metabolism of the largest diazirine-modified sialic acid precursor was so poor that we could not quantify its incorporation level, yet we could readily detect crosslinking of both sialylated glycoproteins and sialylated glycolipids. Notably, our data suggested that photocrosslinking substituent interferes with metabolic crosstalk between GlcNAc and ManNAc pathways, resulting in faithful incorporation of the diazirine into only sialylated glycoconjugates. In addition to these findings, we note that our ability to detect a crosslinked CTxB-GM1a complex by mass spectrometry provides a blueprint for future efforts to use photocrosslinking for binding partner discovery.

Supplementary Material

Refer to Web version on PubMed Central for supplementary material.

Acknowledgments

We thank Kim Orth (UT Southwestern Medical Center) for sharing Jurkat cells, Michael Pawlita (German Cancer Research Center) and James Paulson (The Scripps Research Institute) for sharing BJA-B K20, BJA-B K88 cells, and Ellen Vitetta (UT Southwestern Medical Center) for sharing Daudi cells. We thank Peter Vu (UT Southwestern Medical Center) for sharing reagents. We thank Yan Li (UT Southwestern Medical Center Protein Chemistry Technology Center) for mass spectrometry analysis of sugars, Angela Mobley (UT Southwestern Medical Center Flow Cytometry Core Facility) for help with flow cytometry, Luke Rice (UT Southwestern Medical Center) for

access to the ultracentrifuge, and Wen-hong Li (UT Southwestern Medical Center) for access to the HPLC with a fluorescence detector. We also thank Yoshihito Tanaka and Chad M. Whitman for helpful discussions and suggestions. We acknowledge the following funding sources: the National Institutes of Health (GM090271), the March of Dimes (5-FY06-913), the Welch Foundation (I-1686), and the University of Texas Southwestern Medical Center. This content is solely the responsibility of the authors and does not necessarily represent the official views of the National Institute of General Medical Sciences or the National Institutes of Health. M. R. B. acknowledges the support of an NSF Graduate Research Fellowship and of Stanford University. J. J. K. is an Alfred P. Sloan Research Fellow.

References

1. Sinclair AM, Elliott S. Glycoengineering: The effect of glycosylation on the properties of therapeutic proteins. J. Pharm. Sci. 2005; 94:1626–1635. [PubMed: 15959882]
2. Schauer R. Sialic acids as regulators of molecular and cellular interactions. Curr. Opin. Struct. Biol. 2009; 19:507–514. [PubMed: 19699080]
3. Varki A. Glycan-based interactions involving vertebrate sialic-acid-recognizing proteins. Nature. 2007; 446:1023–1029. [PubMed: 17460663]
4. McEver RP, Moore KL, Cummings RD. Leukocyte trafficking mediated by selectin-carbohydrate interactions. J. Biol. Chem. 1995; 270:11025–11028. [PubMed: 7538108]
5. Holmgren J, Lönnroth I, Månsson J, Svennerholm L. Interaction of cholera toxin and membrane GM1 ganglioside of small intestine. Proc. Natl. Acad. Sci. U. S. A. 1975; 72:2520–2524. [PubMed: 1058471]
6. Connor RJ, Kawaoka Y, Webster RG, Paulson JC. Receptor specificity in human, avian, and equine H2 and H3 influenza virus isolates. Virology. 1994; 205:17–23. [PubMed: 7975212]
7. Varki NM, Varki A. Diversity in cell surface sialic acid presentations: implications for biology and disease. Lab. Invest. 2007; 87:851–857. [PubMed: 17632542]
8. Du J, Meledeo MA, Wang Z, Khanna HS, Paruchuri VDP, Yarema KJ. Metabolic glycoengineering: Sialic acid and beyond. Glycobiology. 2009; 19:1382–1401. [PubMed: 19675091]
9. Tanaka Y, Kohler JJ. Photoactivatable crosslinking sugars for capturing glycoprotein interactions. J. Am. Chem. Soc. 2008; 130:3278–3279. [PubMed: 18293988]
10. Han S, Collins BE, Bengtson P, Paulson JC. Homomultimeric complexes of CD22 in B cells revealed by protein-glycan cross-linking. Nat. Chem. Biol. 2005; 1:93–97. [PubMed: 16408005]
11. Luchansky SJ, Goon S, Bertozzi CR. Expanding the diversity of unnatural cell-surface sialic acids. Chembiochem. 2004; 5:371–374. [PubMed: 14997530]
12. Ramya TNC, Weerapana E, Liao L, Zeng Y, Tateno H, Liao L, Yates JR, Cravatt BF, Paulson JC. *In situ trans* ligands of CD22 identified by glycan-protein photocross-linking-enabled proteomics. Mol. Cell. Prot. 2010; 9:1339–1351.
13. Bond MR, Whitman CM, Kohler JJ. Metabolically incorporated photocrosslinking sialic acid covalently captures a ganglioside-protein complex. Mol. Biosys. 2010; 6:1796–1799.
14. Tanaka Y, Bond MR, Kohler JJ. Photocrosslinkers illuminate interactions in living cells. Mol. Biosys. 2008; 4:473–480.
15. Bayley, H. Photogenerated Reagents in Biochemistry and Molecular Biology. Elsevier; 1983.
16. Bond MR, Zhang H, Vu PD, Kohler JJ. Photocrosslinking of glycoconjugates using metabolically incorporated diazirine-containing sugars. Nat. Prot. 2009; 4:1044–1063.
17. Saxon E, Bertozzi CR. Cell surface engineering by a modified Staudinger reaction. Science. 2000; 287:2007–2010. [PubMed: 10720325]
18. Patrie SM, Mrksich M. Self-assembled monolayers for MALDI-TOF mass spectrometry for immunoassays of human protein antigens. Anal. Chem. 2007; 79:5878–5887. [PubMed: 17602570]
19. Jones MB, Teng H, Rhee JK, Lahar N, Baskaran G, Yarema KJ. Characterization of the cellular uptake and metabolic conversion of acetylated N-acetylmannosamine (ManNAc) analogues to sialic acids. Biotech. Bioeng. 2004; 85:394–405.
20. Sarkar AK, Rostand KS, Jain RK, Matta KL, Esko JD. Fucosylation of disaccharide precursors of sialyl Lewis(X) inhibit selectin-mediated cell adhesion. J. Biol. Chem. 1997; 272:25608–25616. [PubMed: 9325281]

21. Luchansky SJ, Yarema KJ, Takahashi S, Bertozzi CR. GlcNAc 2-epimerase can serve a catabolic role in sialic acid metabolism. J. Biol. Chem. 2003; 278:8035–8042. [PubMed: 12499362]
22. Keppler OT, Hinderlich S, Langner J, Schwartz-Albiez R, Reutter W, Pawlita M. UDP-GlcNAc 2-epimerase: A regulator of cell surface sialylation. Science. 1999; 284:1372–1376. [PubMed: 10334995]
23. Keppler OT, Peter ME, Hinderlich S, Moldenhauer G, Stehling P, Schmitz I, Schwartz-Albiez R, Reutter W, Pawlita M. Differential sialylation of cell surface glycoconjugates in a human B lymphoma cell line regulates susceptibility for CD95 (APO-1/Fas)-mediated apoptosis and for infection by a lymphotropic virus. Glycobiology. 1999; 9:557–569. [PubMed: 10336988]
24. Luchansky SJ, Argade S, Hayes BK, Bertozzi CR. Metabolic functionalization of recombinant glycoproteins. Biochemistry. 2004; 43:12358–12366. [PubMed: 15379575]
25. Chokhawala HA, Huang SS, Lau K, Yu H, Cheng JS, Thon V, Hurtado-Ziola N, Guerrero JA, Varki A, Chen X. Combinatorial chemoenzymatic synthesis and high-through put screening of sialosides. ACS Chem. Biol. 2008; 3:567–576. [PubMed: 18729452]
26. Brinkman-Van der Linden ECM, Sonnenburg JL, Varki A. Effects of sialic acid substitutions on recognition by *Sambucus nigra* agglutinin and *Maackia amurensis* hemagglutinin. Anal. Biochem. 2002; 303:98–104. [PubMed: 11906157]
27. Zeng Y, Ramya TNC, Dirksen A, Dawson PE, Paulson JC. High-efficiency labeling of sialylated glycoproteins on living cells. Nat. Meth. 2009; 6:207–209.
28. Shibuya N, Goldstein IJ, Broekaert WF, Nsimba-Lubaki M, Peeters B, Peumans WJ. The elderberry (*Sambucus nigra* L.) bark lectin recognizes the Neu5Ac(α2-6)Gal/GalNAc sequence. J. Biol. Chem. 1987; 262:1596–1601. [PubMed: 3805045]
29. Wang WC, Cummings RD. The immobilized leukoagglutinin from the seeds of *Maackia amurensis* binds with high affinity to complex-type Asn-linked oligosaccharides containing terminal sialic acid-linked alpha-2,3 to penultimate galactose residues. J. Biol. Chem. 1988; 263:4576–4585. [PubMed: 3350806]
30. Geisler C, Jarvis DL. Letter to the Glyco-Forum: Effective glycoanalysis with *Maackia amurensis* lectins requires a clear understanding of their binding specificities. Glycobiology. 2011; 21:988–993. [PubMed: 21863598]
31. Iglesias JL, Lis H, Sharon N. Purification and properties of a D-galactose/N-acetyl-D-galactosamine-specific lectin from *Erythrina cristagalli*. Eur. J. Biochem. 1982; 123:247–252. [PubMed: 6978812]
32. Brooks SA. The involvement of *Helix pomatia* lectin (HPA) binding N-acetylgalactosamine glycans in cancer progression. Histol. Histopathol. 2000; 15:143–158. [PubMed: 10668205]
33. Hara S, Yamaguchi M, Takemori Y, Furuhata K, Ogura H, Nakamura M. Determination of mono-O-acetylated N-acetylneuraminic acids in human and rat sera by fluorometric high-performance liquid chromatography. Anal. Biochem. 1989; 179:162–166. [PubMed: 2757191]
34. Nakamura, M. H., Shuuji; Yamaguchi, Masatoshi; Takemori, Yasuyo; Ohkura, Yosuke. 1,2-diamino-4,5-methylenedioxybenzene as a highly sensitive fluorogenic reagent for α-keto acids. Chem. Pharm. Bull. 1987; 35:687–692.
35. Yu S-H, Bond MR, Whitman CM, Kohler JJ. Metabolic labeling of glycoconjugates with photocrosslinking sugars. Methods Enz. 2010; 478:541–562.
36. Bussink AP, van Swieten PF, Ghauharali K, Scheij S, van Eijk M, Wennekes T, van der Marel GA, Boot RG, Aerts JMFG, Overkleeft HS. N-azidoacetylmannosamine-mediated chemical tagging of gangliosides. J. Lipid Res. 2007; 48:1417–1421. [PubMed: 17392268]
37. Chefalo P, Pan Y, Nagy N, Guo Z, Harding CV. Efficient metabolic engineering of GM3 on tumor cells by N-phenylacetyl-D-mannosamine. Biochemistry. 2006; 45:3733–3739. [PubMed: 16533056]
38. Wang Q, Zhang J, Guo Z. Efficient glycoengineering of GM3 on melanoma cell and monoclonal antibody-mediated selective killing of the glycoengineered cancer cell. Bioorg. Med. Chem. 2007; 15:7561–7567. [PubMed: 17892942]
39. Zou W, Borrelli S, Gilbert M, Liu T, Pon RA, Jennings HJ. Bioengineering of surface GD3 ganglioside for immunotargeting human melanoma cells. J. Biol. Chem. 2004; 279:25390–25399. [PubMed: 15047693]

40. Pan Y, Chefalo P, Nagy N, Harding C, Guo Z. Synthesis and immunological properties of N-modified GM3 antigens as therapeutic cancer vaccines. J. Med. Chem. 2005; 48:875–883. [PubMed: 15689172]
41. Whitman CM, Yang F, Kohler JJ. Modified GM3 gangliosides produced by metabolic oligosaccharide engineering. Bioorg. Med. Chem. Lett. in press.
42. Ladisch S, Gillard B. A solvent partition method for microscale ganglioside purification. Anal. Biochem. 1985; 146:220–231. [PubMed: 3993932]
43. Schnaar RL. Isolation of glycosphingolipids. Methods Enz. 1994; 230:348–370.
44. Lai CY. Determination of the primary structure of cholera toxin B subunit. J. Biol. Chem. 1977; 252:7249–7256. [PubMed: 903362]
45. Williams JP, Smith DC, Green BN, Marsden BD, Jennings KR, Roberts LM, Scrivens JH. Gas phase characterization of the noncovalent quaternary structure of cholera toxin and the cholera toxin B subunit pentamer. Biophys. J. 2006; 90:3246–3254. [PubMed: 16461395]
46. Jacobs CL, Goon S, Yarema KJ, Hinderlich S, Hang HC, Chai DH, Bertozzi CR. Substrate specificity of the sialic acid biosynthetic pathway. Biochemistry. 2001; 40:12864–12874. [PubMed: 11669623]
47. Keppler OT, Herrmann M, von der Lieth CW, Stehling P, Reutter W, Pawlita M. Elongation of the N-acyl side chain of sialic acids in MDCK II cells inhibits influenza A virus infection. Biochem. Biophys. Res. Commun. 1998; 253:437–442. [PubMed: 9878554]
48. Oetke C, Brossmer R, Mantey LR, Hinderlich S, Isecke R, Reutter W, Keppler OT, Pawlita M. Versatile biosynthetic engineering of sialic acid in living cells using synthetic sialic acid analogues. J. Biol. Chem. 2002; 277:6688–6695. [PubMed: 11751912]
49. Saxon E, Luchansky SJ, Hang HC, Yu C, Lee SC, Bertozzi CR. Investigating cellular metabolism of synthetic azidosugars with the Staudinger ligation. J. Am. Chem. Soc. 2002; 124:14893–14902. [PubMed: 12475330]
50. Middaugh CR, Vanin EF, Ji TH. Chemical crosslinking of cell membranes. Mol. Cell. Biochem. 1983; 50:115–141. [PubMed: 6855747]
51. Harduin-Lepers A, Vallejo-Ruiz V, Krzewinski-Recchi MA, Samyn-Petit B, Julien S, Delannoy P. The human sialyltransferase family. Biochimie. 2001; 83:727–737. [PubMed: 11530204]
52. Datta AK. Comparative sequence analysis in the sialyltransferase protein family: Analysis of motifs. Current Drug Targets. 2009; 10:483–498. [PubMed: 19519350]
53. Baumann H, Doyle D. Turnover of plasma membrane glycoproteins and glycolipids of hepatoma tissue culture cells. J. Biol. Chem. 1978; 253:4408–4418. [PubMed: 207700]
54. Tettamanti G. Ganglioside/glycosphingolipid turnover: new concepts. Glycoconj. J. 2004; 20:301–317. [PubMed: 15229395]

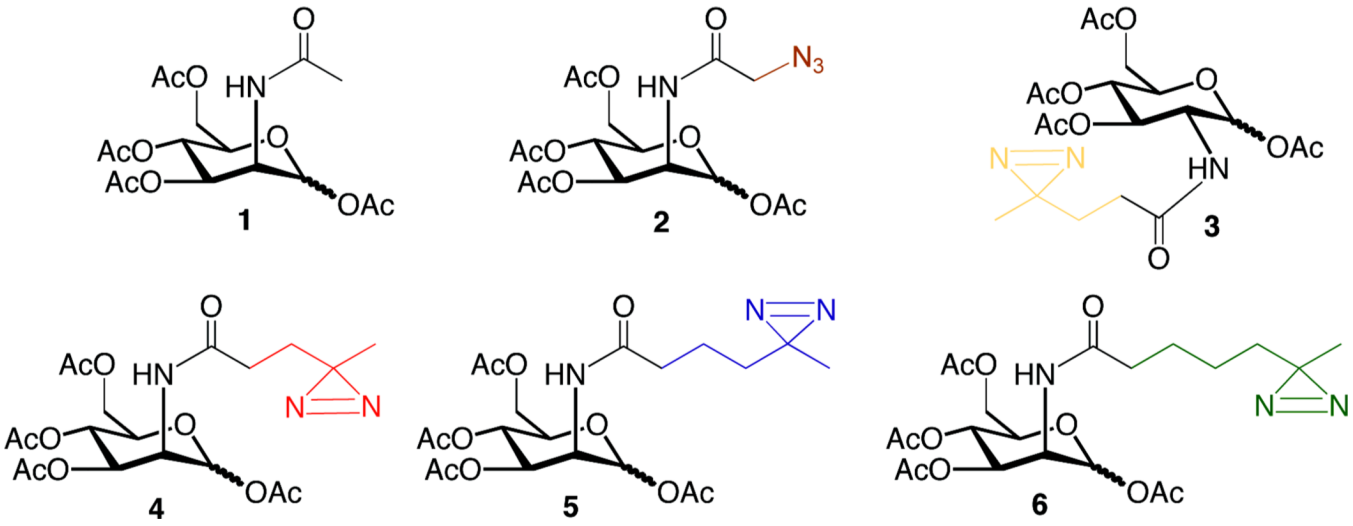

Figure 1. Per-*O*-acetylated *N*-acyl hexosamines

The *N*-acyl side chains of ManNAc and *N*-acetylglucosamine (GlcNAc) analogs were modified by the addition of a diazirine or an azide. Ac_4ManNAc (**1**) is a protected form of naturally occurring ManNAc. Ac_4ManNAz (**2**) is an azide-containing analog that is metabolized to sialosides with high efficiency [24]. The names of the diazirine-modified sugars (**3**–**6**) are derived from the number of methylene groups separating the carbonyl and diazirine on the *N*-acyl side chain: Ac_4GlcNDAz(2me) (**3**), Ac_4ManNDAz(2me) (**4**), Ac_4ManNDAz(3me) (**5**), and Ac_4ManNDAz(4me) (**6**).

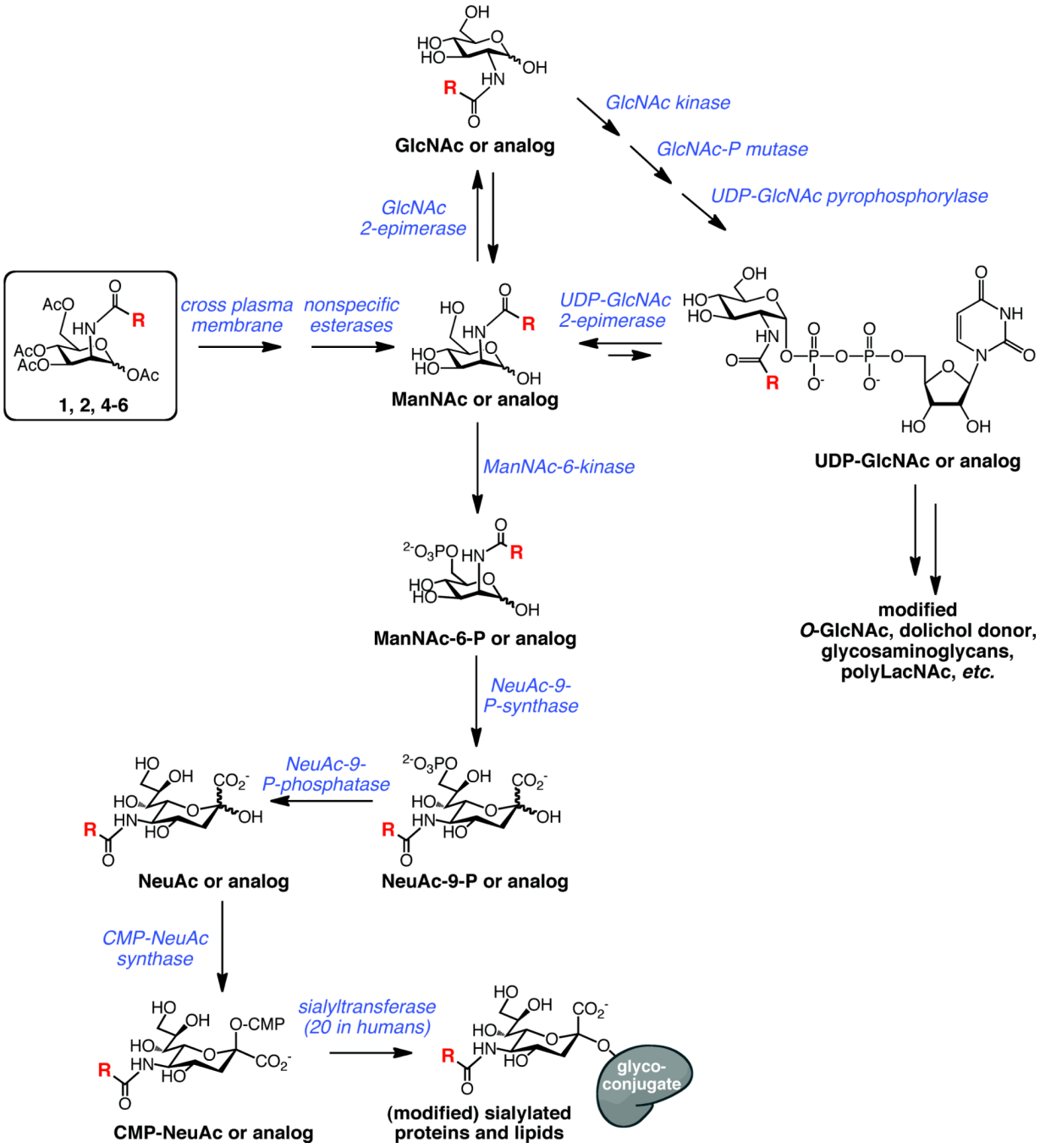

Figure 2. Metabolism of ManNAc and ManNAc analogs

Per-*O*-acetylated ManNAc analogs (boxed) diffuse across the plasma membrane after which acetyl groups are cleaved by nonspecific esterases. R is -CH_3 for naturally occurring ManNAc. ManNAc and analogs can be converted to the corresponding sialosides by a series of enzymatic transformations. Alternative possible fates for ManNAc analogs include conversion to GlcNAc analogs and UDP-GlcNAc analogs that are precursors for other glycoconjugates.

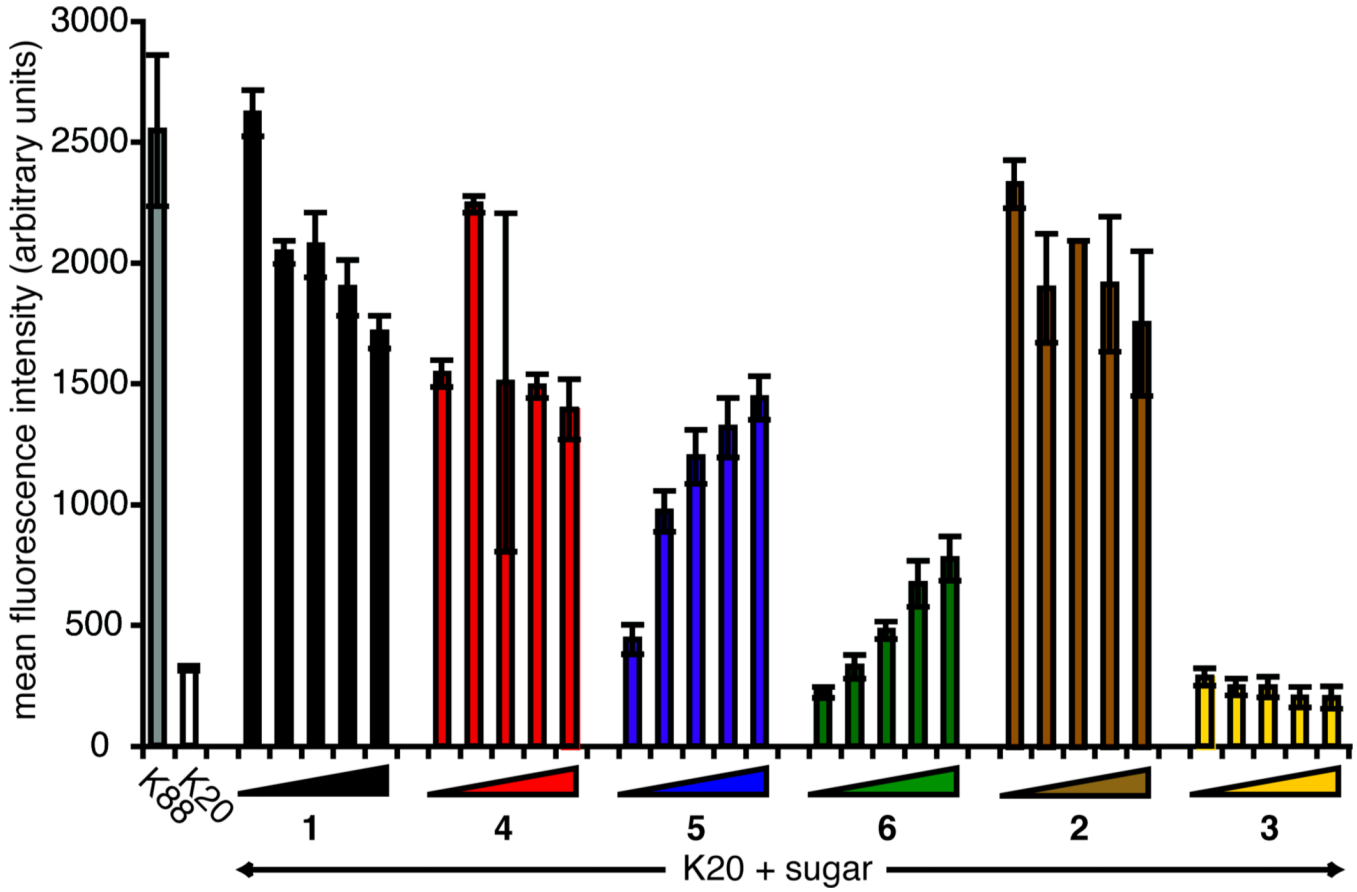

Figure 3. Metabolism of compounds to cell surface α2–6-linked sialic acids

BJA-B K20 cells were treated with increasing concentrations (10, 50, 100, 200, and 300 μM) of Ac_4ManNAc, Ac_4ManNAc analogs, or Ac_4GlcNDAz(2me). Cell surface α2–6-linked sialic acid levels of BJA-B K88 and K20 cells were assessed by SNA-FITC binding, as measured by flow cytometry. The standard deviation represents technical duplicate samples. Two biological replicates of the experiment were performed, yielding similar data (not shown).

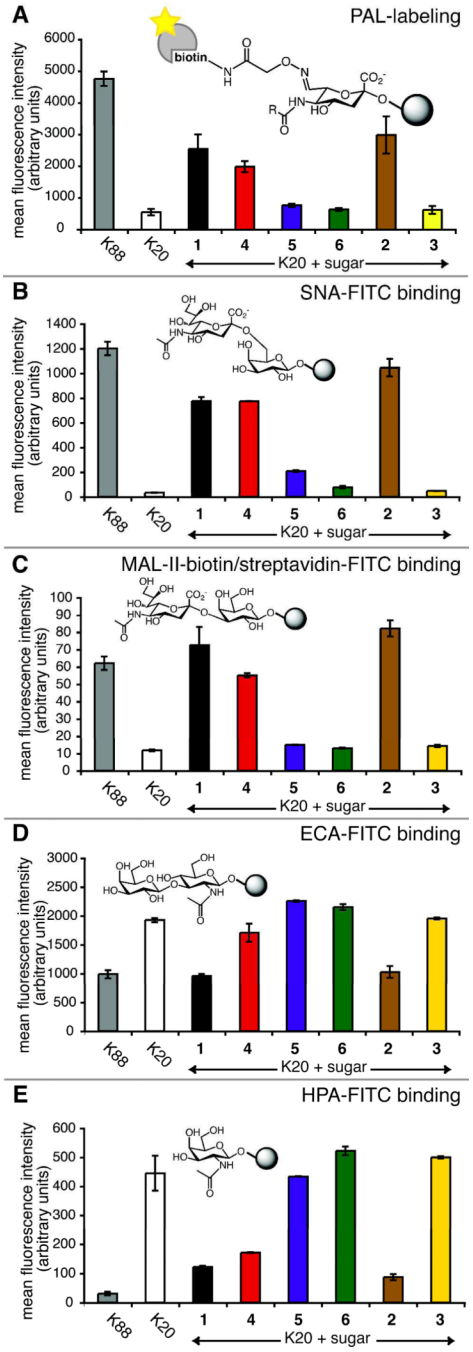

Figure 4. Cell surface sialic acid measured by flow cytometry

BJA-B K20 cells were grown in serum-free media supplemented with 100 μM **1–6**. (A) Total sialic acid detected by PAL; (B) Siaα2–6 galactose (Siaα2–6Gal) epitope detected by SNA lectin; (C) Siaα2–3Gal epitope detected by MAL-II lectin; (D) unsialylated terminal *N*-acetyllactosamine (LacNAc) detected by ECA lectin; (E) unsialylated terminal *N*-acetylgalactosamine (GalNAc) detected by HPA lectin. Error bars represent the standard deviation for three technical replicates.

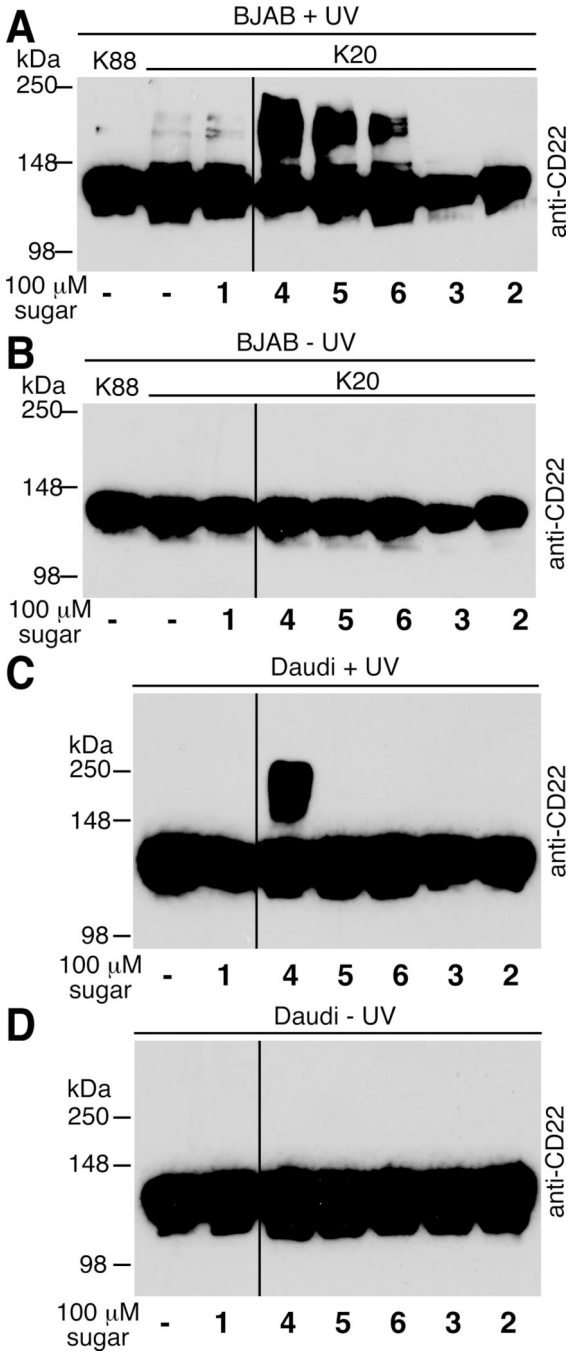

Figure 5. Photocrosslinking of Siglec CD22 in BJA-B K20 and Daudi cells

BJA-B K20 or Daudi cells were cultured with photocrosslinking sugars, photoirradiated, and lysed. Lysates from BJA-B K20 cells cultured with diazirine-containing sugars and exposed to UV light (A) or no UV light (B). Lysates from Daudi cells cultured with diazirine-containing sugars and exposed to UV light (C) or no UV light (D). For all blots, β-actin was used as a control to demonstrate similar levels of protein loading in every lane (data not shown).

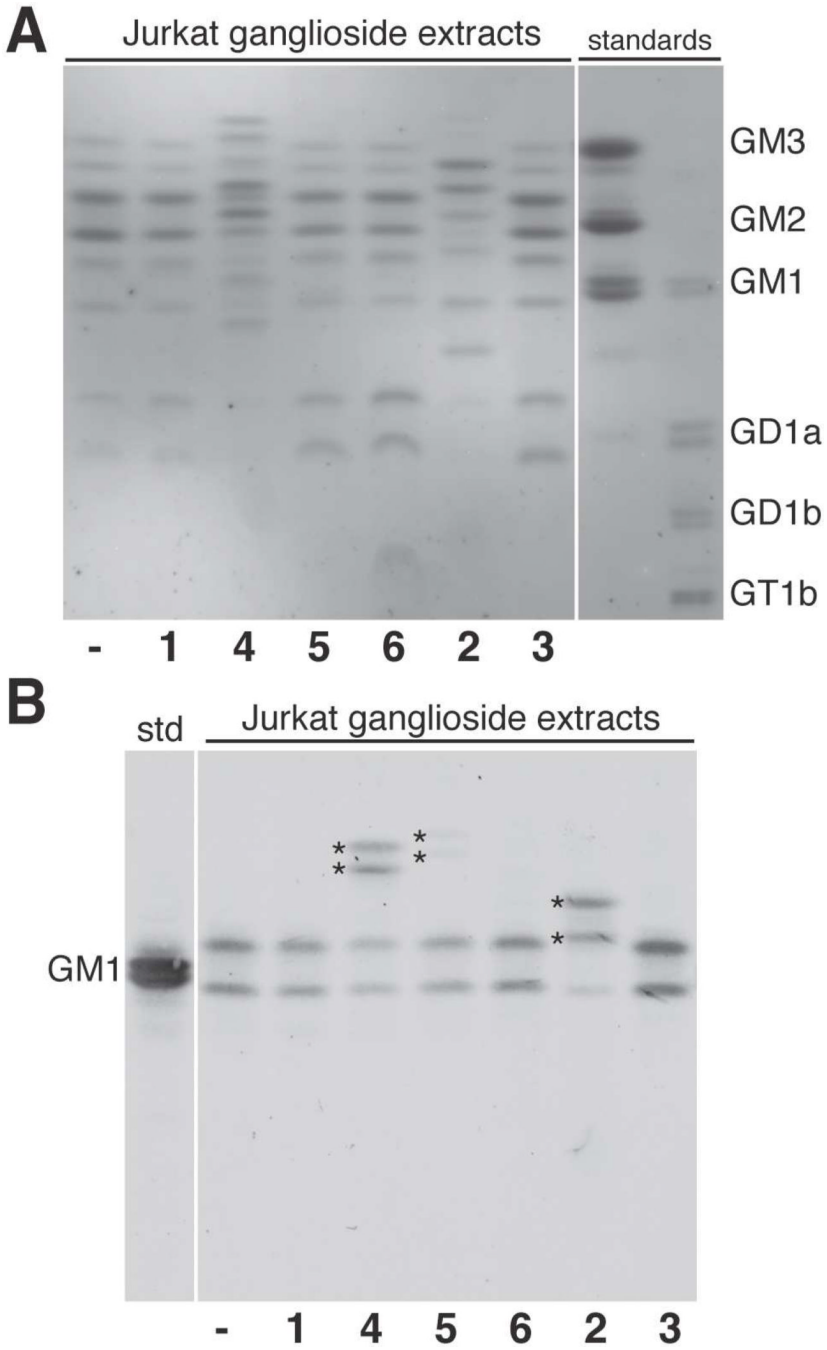

Figure 6. HPTLC analysis of gangliosides extracted from cultured Jurkat cells

Jurkat cells were cultured alone or with **1–6**. (A) The HPTLC plate was stained for sialic acid using resorcinol. Jurkat cells produce a variety of gangliosides: GM3, GM2, GM1a, and GD1a. The pattern of gangliosides changed upon introduction of unnatural sialic acid precursors Ac_4ManNDAz(2me) and Ac_4ManNAz, but not other compounds. (B) The HPTLC plate was probed with CTxB-488, which recognizes ganglioside GM1a. Naturally occurring GM1a molecules are present in all ganglioside extracts. Additional species with CTxB-488 reactivity (s⋆) appeared when cells were cultured with Ac_4ManNDAz(2me), Ac_4ManNDAz(3me), or Ac_4ManNAz.

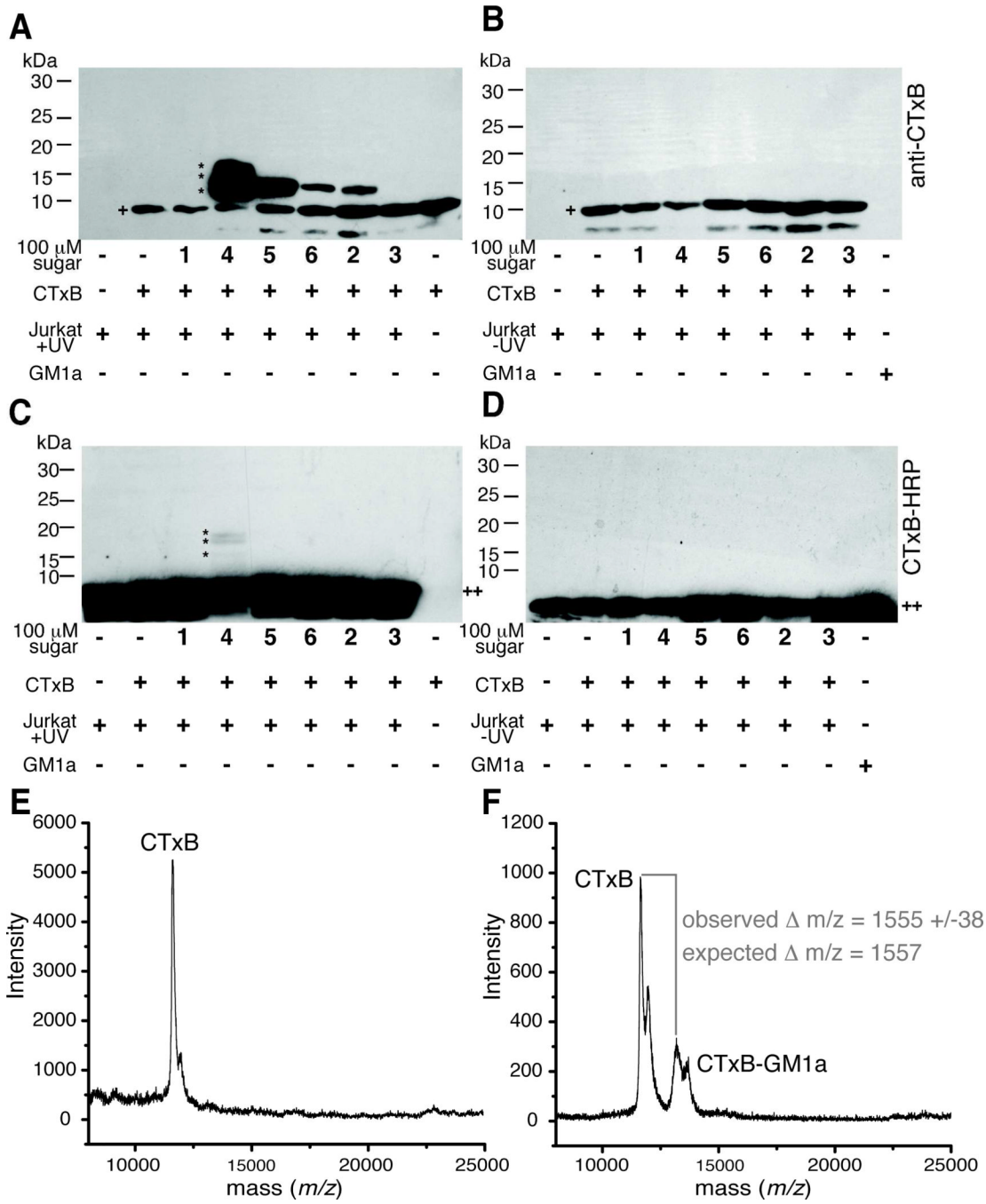

Figure 7. Photocrosslinking sugar analogs covalently capture CTxB-GM1a interaction

Jurkat cells were cultured with or without sugar analogs **1–6** for 72 hours and then incubated with CTxB for 45 min at 4 °C. Cells were photoirradiated, lysed, and the lysates separated by reducing SDS-PAGE followed by protein transfer to PVDF membranes. UV-irradiated (A) and non-UV-irradiated samples (B) were probed for the presence of CTxB (+) using an anti-CTxB antibody. A slower mobility band has an apparent molecular weight consistent with formation of a CTxB-GM1a complex (~13 kDa, *). The identity of the very low molecular weight band (<10 kDa) is not known, but it appears to be related to a contaminant in the CTxB preparation. UV-irradiated (C) and non-UV-irradiated samples (D) were probed for the presence of GM1a (++) using CTxB-HRP. A slower mobility band has an apparent

molecular weight consistent with formation of a CTxB-GM1a complex (~13 kDa, *). Membranes were stripped and probed for β–actin to demonstrate equal protein loading in each lane (not shown). (E) SAMDI-TOF MS spectrum of SAM-bound monomeric CTxB species derived from cells cultured with Ac_4ManNAc, incubated with CTxB, and photoirradiated. (F) SAMDI-TOF MS spectrum of SAM-bound monomeric CTxB and crosslinked CTxB-GM1a-SiaDAz(2me) derived from cells cultured with Ac_4ManNDAz(2me), incubated with CTxB, and photoirradiated.

Table 1

DMB-derivatization of sialic acids reveals that SiaDAz(2me) and SiaDAz(3me) effectively compete with endogenous sialic acid for incorporation into glycoconjugates

Jurkat cells were cultured with the indicated compounds, harvested and fractionated. Sialic acids were derivatized by DMB and separated by reverse phase HPLC with fluorescence detection (see Figures S4–S6). Peaks were integrated to derive the percentages of Neu5Ac and other sialic acids. Multiple values indicate results from independent experiments. N.D. indicates that a peak corresponding to SiaDAz(4me) could not be identified.

compound added	fraction analyzed	% of total sialic acid	
		Neu5Ac	SiaDAz (2me, 3me, or 4me)
no added sugar	cytosol	100	0
	membrane	100	0
Ac_4ManNAc	cytosol	100	0
	membrane	100	0
Ac_4ManNDAz(2me)	cytosol	15	85
	membrane	26	74
Ac_4ManNDAz(3me)	cytosol	63, 70	37, 30
	membrane	92, 96	8, 4
Ac_4ManNDAz(4me)	cytosol	100	N.D.
	membrane	100	N.D.